IEEE Access
Multidisciplinary | Rapid Review | Open Access Journal

Received July 31, 2019, accepted August 8, 2019, date of publication August 13, 2019, date of current version August 28, 2019.

Digital Object Identifier 10.1109/ACCESS.2019.2935024

Performance Analysis of Frequency Hopping Ad Hoc Communication System With Non-Orthogonal Multiple Access

SHAOSHENG LI, HONGRUI NIE, AND HUICI WU
Beijing University of Posts and Telecommunications, Beijing 100876, China

Corresponding author: Shaosheng Li (lss@bupt.edu.cn)

This work was supported in part by the project of the Beijing Municipal Science and Technology Commission under Grant Z181100003218015, and in part by the Fundamental Research Funds for the Central Universities.

ABSTRACT In this paper, we investigate the downlink performance of frequency hopping Ad Hoc communication system with non-orthogonal multiple access (FH-NOMA Ad Hoc), in which the mobile users are divided into multiple groups defined as NOMA clusters. Each NOMA cluster works on a certain frequency resource block with frequency hopping. Each mobile user in a NOMA cluster can act as NOMA transmitter with equal access probability and serve the rest mobile users with differentiated power allocation. With the considered network model, a stochastic geometry framework is provided to analyze the coverage and data rate performance of the FH-NOMA Ad Hoc network. Expressions for the coverage probability and the average data rate of a typical mobile user are derived. Finally, numerical and Monte Carlo simulations are provided to validate the theoretical analysis. The results reveal that the coverage probability of the FH-NOMA Ad Hoc network can be improved by varying the radius of each NOMA cluster, the number of frequency points, the density of NOMA clusters and user power allocation. Importantly, there is a constraint relationship between the density of NOMA clusters and the number of frequency points.

INDEX TERMS Ad Hoc, frequency hopping, non-orthogonal multiple access, stochastic geometry.

I. INTRODUCTION

Ad Hoc communication system is widely acknowledged as the main network architecture in emergency, military and some other flexible communication scenarios due to its flexibility, scalability and rapid deployment. The existence of interference degrades the network performance seriously. Blocking interference, one of the most serious interference attacks, can cause serious communication interruption and thus provide poor coverage performance and low network throughput of the Ad Hoc network. Frequency Hopping (FH) can effectively resist the external strong blocking interference due to its FH processing gain by constantly changing its radio frequency [1], [2] to improve communication quality. Under a certain bit error rate (BER), the FH communications system considering spreading spectrum and Reed-Solomon (RS) concatenated coding [3], [4] can have high reliability even if one third of the available frequency is blocked. [5] provides numerical and simulation results of a FH system's upper bound on bit error rate (BER) under some attack, including partial-band jamming resistance for communication, which has the similar BER performance as conventional FH system.

However, the network capacity of the FH communication system is restricted since FH communication cannot transmit information during the period of frequency change, which results in low valid bit rate compared with fixed frequency communication [6]. Thus, the main problem of the FH communication system in emergency communication is how to improve the system capacity.

Non-Orthogonal Multiple-Access (NOMA) [7], as a novel multiple access multiplexing technique in the fifth generation (5G) mobile networks, can provide high network capacity by multiplexing multiple users in a frequency block resource with differentiated power level at the transmitter and successive interference cancellation (SIC) at the receivers. Leveraging NOMA in the FH Ad Hoc communication networks, multiple mobile users can share the same frequency resource block. Motivated by this, we propose the model

The associate editor coordinating the review of this article and approving it for publication was Yuanwei Liu.

of FH-NOMA Ad Hoc communication system based on practical emergency communication systems, requiring high system capacity as well as high anti-jamming ability.

A. RELATED WORKS

The advent of the first FH radio station from the late 1970s indicated its development. Research on FH technique has significance in the field of military communications. Until now, FH has been considered from a practical perspective in multiple fields [8]–[11]. In addition, the adjacent frequency interference of frequency-hopping radio networks was investigated by Qiao *et al.* [12]. Li *et al.* [13] invoked error probabilities for frequency-Hopping Spread Spectrum Multiple Access (FH-SSMA) Systems in the presence of interference. In addition, El Gamal and Geraniotis [14] proposed comparison between FH/SSMA and DS/CDMA, which argued that synchronous FH/SSMA is implementable and can provide higher capacity than asynchronous DS/CDMA under certain conditions. Both individual optimal frequency-hopping sequences and optimal families of frequency-hopping sequences were presented in Ding *et al.* [15], which improved the anti-interference and security of the FH signal. Importantly, synchronization is one of the key techniques in FH communication system, and multiple synchronization schemes for FH was analyzed by [16]–[18]. Furthermore, Sudha *et al.* [19] proposed the performance improvement of frequency-hopped spread spectrum networks (FHSS) signals by using rate compatible parallel-concatenated block codes using BCH codes. As a further development, FH technique applied to wireless Ad Hoc networks was investigated by Zou *et al.* [16] to solve the safety problem of Ad Hoc network physical layer.

What's more, NOMA has received significant research for its capability to improve spectral efficiency compared with Orthogonal Multiple-Access (OMA). A simple downlink PD-NOMA transmission scheme called Multi-user superposition Transmission (MUST) was used in the Third Generation Partnership Project (3GPP) Long Term Evolution [20]. Benjebbour *et al.* [21] studied that the downlink system using NOMA can achieve an average throughput gain of 30% higher than the tradition OMA technology. The multi-user power allocation, signaling overhead, SIC error propagation, high-speed scene and other issues of the NOMA system were discussed, which provided a reference for further research on NOMA technology. A. Benjebbour considered the random distribution of users in the single-cell downlink NOMA system, and the closed expression of the outage probability was obtained [22]. The results showed that NOMA could obtain better outage performance compared with OMA system if the user 's power factor and target rate were selected properly. Liu *et al.* [23] extended the above results to large-scale cognitive radio networks. The impact of user scheduling on improving NOMA system throughput and cell edge user throughput was investigated by Do *et al.* [24]. P. Swami studied the downlink NOMA user outage probability based on the principle of user fairness [25]. Additionally, a user-power allocation optimization problem was proposed by Krikidis and Timotheous by considering the user fairness of a NOMA system [26]. Moreover, Sun *et al.* [27] considered multiple-input multiple output (MIMO) NOMA systems with two users, providing optimal and low complexity power allocation algorithms within the limitations of total power and weak user's rate to maximize the sum capacity. For maximizing the average received power for mobile users, a NOMA and massive MIMO based user association scheme is developed by Liu *et al.* [28].

B. MOTIVATION

The aforementioned literatures are significant study of FH and NOMA technologies. While the performance of FH Adhoc communication system with NOMA is less well understood, taking into account the anti-interference ability and large-capacity requirements of the emergency communication system. We consider the co-channel interference introduced by NOMA and the self-interference introduced by FH. To investigate the coverage probability and average data rate performance of the considered network, an analytical framework of coverage probability and average data rate is provided with stochastic geometry [29]–[31]. We define the set containing all the mobile users that multiplex the same frequency resource block as a NOMA cluster. Specifically, multiple NOMA clusters are randomly distributed in the 2D plane. For each NOMA cluster, a mobile user acts as the transmitter and the rest mobile users are the receivers. The radio frequencies selection of NOMA clusters are determined by FH pattern. Mathematically, homogeneous Poisson Point Process is applied to model the deployment of FH-NOMA transmitters. The rest mobile users (receivers) of a FH-NOMA cluster are located uniformly at random in a disc around transmitter. Different FH hopping patterns are applied in the NOMA clusters, which introduce inter-cluster interference due to frequency collisions. The sum of interference power at each receiver should not exceed a peak threshold. Based on the formulated mathematical model, the coverage probability and average data rate can be exploited, since the location of receivers served by the same transmitter and FH-NOMA clusters in the network is not known in advance. In the recent research, there is no relevant framework for exploring FH Adhoc communication system with NOMA.

C. CONTRIBUTIONS AND ORGANIZATION

In this paper, we propose a framework of FH Adhoc communication system with NOMA to improve anti-jamming ability and system capacity. We apply homogeneous poisson point processes (PPPs) to model the location of FH-NOMA transmitters. The rest FH-NOMA mobile users (receivers) served by the same transmitter are located around the parent mobile user (transmitter) randomly, uniformly and independently. In addition, we consider the distance order of the receivers in a typical FH-NOMA cluster. In this model, we analyze the intra-interference introduced by NOMA and inter-interference introduced by FH. We derive expressions

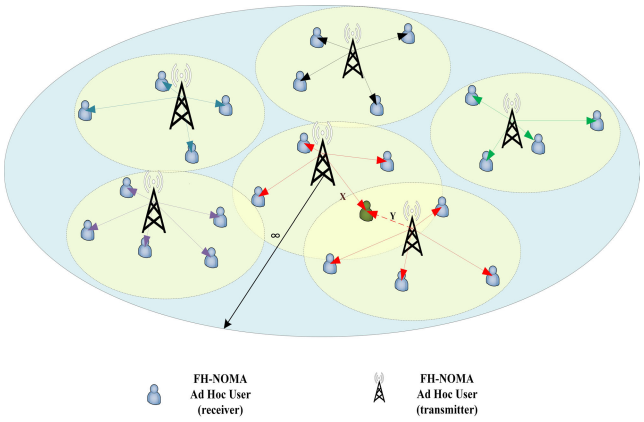

FIGURE 1. Network model for FH NOMA transmission in single-antenna scenario.

for coverage probability of a typical receiver and average data rate of mobile users within a typical cluster.

Finally, numerical and simulation results are provided to validate the theoretical analysis and to demonstrate the impact of the key system parameters including the radius of each FH-NOMA cluster, the number of available frequency points, the density of deployment of NOMA clusters and user power allocation. The results reveal that the coverage probability can be improved by reducing the area of each NOMA cluster, increasing the number of frequency points and deploying NOMA clusters more densely. However, the number of the frequency points directly determine the number of links which limits the cluster density. For a given number of frequency points, the system capacity suddenly decreases when the cluster density reach its upper bound.

The rest of this paper is organized as follows. In Section II,the frequency hopping NOMA Ad Hoc network scenario is proposed, including system model, frequency reuse and propagation model. In Section III, the coverage probability and average data rate of the considered network are analyzed and derived, which relies on the typical receiver in the typical cluster. The numerical results are presented in Section IV which is followed by the conclusion in Section V.

II. SYSTEM MODEL

In this section, the network layout, channel reuse and wireless propagation model are introduced.

A. NETWORK LAYOUT

As illustrated in Fig.1, a FH-NOMA Ad Hoc communication system is considered, where the FH-NOMA clusters are deployed in the 2D plane according to Poisson cluster process (PCP) with their centers are distributed as homogeneous PPP Φ with the density λ. In each NOMA cluster, N users are included and each FH-NOMA user have equal probability to be a transmitter and rest become receivers. The transmitter is considered to be located at the center of the cluster and the rest N-1 receivers are uniformly distributed within a disc with radius D. The NOMA transmission protocol is invoked within each cluster, assuming that all users work in the slotted Aloha random access mode and only one user transmit signal in a time slot within a cluster. The probability density function (PDF) of the distance R between transmitter and receivers within the same FH-NOMA cluster is given by

$$f_R(r) = \begin{cases} \dfrac{2r}{D^2}, & 0 < r \le D \\ 0, & otherwise, \end{cases} \tag{1}$$

In a typical FH-NOMA cluster, a typical transmitter TX_0 is located at the origin of the coordinate o. A typical receiver RX_0 is selected among the N-1 receivers, and rest transmitter is denoted by TX. X_0 is the distance between TX_0 and the typical receiver RX_0, $\boldsymbol{X} = \{X_1, X_2, \cdots, X_n, \cdots, X_{N-2}\}$ is the set of random ordering distances between TX_0 and rest receivers within the same clusters and $|Y|$ is the distances between TX and typical receiver RX_0.

Suppose that the transmitter transmits signal to all users within the same cluster under the constraint of total power P_t. It is assumed that the transmitter knows the quality-order of receivers' channel conditions. In many actual environment, the FH-NOMA mobile users are clustered according to business logic without obvious boundary in the physical location. Specifically, all FH-NOMA clusters overlap in the area. Moreover, assuming that all mobile users are equipped with a single antenna, different FH-NOMA transmitters can simultaneously transmit signal sharing the same frequency points set while adopting different independent FH patterns.

B. FREQUENCY REUSE

The law of carrier frequency change in frequency hopping communication is called a frequency hopping pattern. It needs to be changed completely randomly to be irregular, which can strengthen the performance of anti-interference. The FH communication often adopts a hopping pattern with a pseudo-random law [32]. Only the two sides of the communication know the FH pattern while the rival can hardly guess the law of FH.

As shown in the Fig. 2, a FH pattern, in which the horizontal axis is time and the vertical axis is frequency. The time is divided into multiple time slots in units of frequency hopping duration, and the total FH bandwidth is divided into several frequency intervals (or frequency blocks). Each grid represents a time frequency block (TFB). At each time slot, the transmitter adopts frequency channel to transmit the signal controlled by a pseudo-random FH sequence.

In a FH communication system, the FH bandwidth and the number of available frequencies are both preset. For example, the total FH bandwidth is 10 MHz, the number of FH frequency sets is 64 and the channel spacing is 25 kHz. In the 10 MHz bandwidth, the number of available channels is much larger than 64. Considering multiple interference factors such as electromagnetic environmental conditions and hostile interference, one or several frequency tables with 64 frequencies can be formulated.

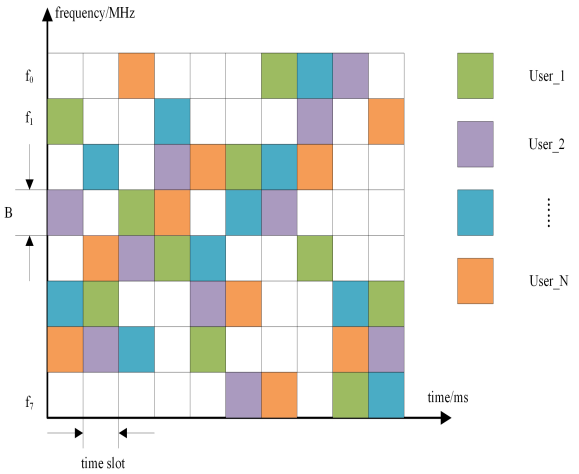

FIGURE 2. Schematic diagram of frequency hopping pattern.

In this paper, the FH asynchronous networking mode is adopted since synchronization has extremely high requirements on timing. The frequency table and the FH pattern are not constrained. This approach does not require all networks to have the same network time reference (NTR). While when the same frequency table is used to form multiple asynchronous networks which are working simultaneously, frequency collisions occur between the asynchronous networks. As long as the FH pattern is well designed, the number of frequency collisions can be controlled within the allowable limits and the overall network system can operate normally. However, the optimal design of the FH sequence is not within the scope of this paper. The FH-NOMA Ad Hoc communication system adopts the random frequency hopping (RFH), which means that the FH-NOMA users randomly select the frequency for FH at each time slot.

Assuming that the number of available frequencies for FH is f, and the hopping codes c can be randomly and independently selected from these f frequencies. Hence the probability that the frequency is selected is $\Pr(c = f_i) = \frac{1}{f}$. Then the probability of a frequency collision between FH-NOMA clusters is

$$q = 1 - (1 - \frac{1}{f})^{M-1}, \tag{2}$$

where the number of available frequencies for FH is f and the number of active FH-NOMA clusters working simultaneously in the FH network is $M = \lambda\pi R_c^2$, and the other $M-1$ clusters are interference sources.

C. WIRELESS CHANNEL MODEL

Signal propagation model is considered to be a composite of path loss and quasi-static Rayleigh fading, where the channel coefficients are constant for each transmission block but independent between different transmission block. In other words, the channel coefficients $|h|^2$ is an independent random variable. In the NOMA transmission protocol, it utilizes the difference between different user channel gains, and multiple users are multiplexed in the power domain and orthogonally scheduled at the transmitter, afterwards, they are transmitted on the same TFB. The different power allocation coefficients are assigned to FH-NOMA receivers, and the power allocation coefficients $\{\boldsymbol{a_n^2}\}$ $(0 \le n \le N-1)$ satisfy the conditions that $|a_0|^2 + |a_1|^2 + \cdots + |a_n|^2 + \cdots + |a_{N-2}|^2 = 1$. Both the small scale fading and the path loss are incorporated into the ordered channel gain.

As a consequence, the superposed information sent by a typical FH-NOMA transmitter TX_0 to rest users within the same NOMA cluster is given by

$$\mathcal{X} = \sqrt{p_0}x_0 + \sqrt{p_1}x_1 + \cdots + \sqrt{p_n}x_n + \cdots + \sqrt{p_{N-2}}x_{N-2}, \tag{3}$$

where p_n is the power allocated to receivers. The receiver RX_n with good channel quality is assumed to be capable of cancelling the interference of the user RX_m with poor channel quality using SIC techniques $(n < m \le N-1)$.

The NOMA downlink communication allocates a higher transmission power for users with poor channel quality and lower transmission power for users with good channel quality, so that in a given NOMA cluster, the main interference received by the user comes from users with worse channel quality. Hence the combination of signal at typical receiver which is the n-th closest receiver RX_n within the typical cluster is expressed as

$$y^{(n)} = \underbrace{\sqrt{P_t}a^{(n)}\left|h_{T_0,R_0}\right|\left|X^{(n)}\right|^{-\alpha}\cdot x^{(n)}}_{\textbf{Information signal}} + \underbrace{\sum_{i=1}^{n-1} a^{(i)}\sqrt{P_t}\left|h_{T_0,R_0}\right|\left|X^{(n)}\right|^{-\alpha}\cdot x^{(i)} + w^{(n)}}_{\textbf{Interference and noise signal}}, \tag{4}$$

where P_t is the signal power from transmitter TX_0 and $w^{(n)}$ is the additive white Gaussian noise (AWGN) at n-th user with mean 0 and variance σ^2. In addition, h_{T_0,R_0} is defined as the small-scales rayleigh fading coefficient associated with $h_{T_0,R_0} \sim \mathcal{CN}(0,1)$. $\ell(|X^{(n)}|) = |X^{(n)}|^{-\alpha}$ is the path loss between the typical transmitter and the according the typical receiver RX_0, and α is the path loss exponent. Importantly, $|X^{(n)}|$ is the distance between typical transmitter and the according typical receiver which is n-th closest receiver. The new incremental ordering distance set $\boldsymbol{X'} = \{X^{(1)}, X^{(2)}, \cdots, X^{(n)}, \cdots, X^{(N-1)}\}$ is obtained by ordering the set $\boldsymbol{X}$. Moreover, $\left\{(\boldsymbol{a^{(n)}})^{\boldsymbol{2}}\right\}$ $(1 \le n \le N-1)$ is an incremental ordering set after sorting the set $\{\boldsymbol{a_n^2}\}$ $(0 \le n \le N-2)$, and $(a^{(n)})^2$ represents the power allocation coefficient of n-th closest receiver.

III. ANALYSIS OF COVERAGE PROBABILITY AND THE AVERAGE TRANSMISSION DATA RATE

In this section, we focus our attention on analyzing the coverage probability and average data rate of a typical user within a typical clusters based on distance ordering.

A. COVERAGE PROBABILITY

The coverage probability is defined as the probability that a typical receiver received signal-to-interference-plus-noise ratio (SINR) is above pre-determined threshold β, i.e.

$$P(\beta) = \Pr\{\gamma \geq \beta\}, \tag{5}$$

At a typical FH-NOMA receiver RX_0, the received SINR for the according TX_0 can be expressed as

$$\gamma = \frac{S}{I_{in} + I_{out} + \sigma^2}, \tag{6}$$

where S, I_{in} and I_{out} refer to the power of the desired signal, the aggregated signal strength of intra-interference caused by users within the same cluster and inter-cluster interference caused by transmitters in the other clusters using the same frequency point respectively. And σ^2 is additive white Gaussian noise (AWGN) power. I_{in} and I_{out} are independent since they are from different sources.

Applying the total probability formula, the coverage probability can be re-expressed as

$$P(\beta) = Q_1 P_{(1)} + \cdots + Q_n P_{(n)} + \cdots + Q_{N-1} P_{(N-1)}, \tag{7}$$

where Q_n is the probability of the typical receiver being the n-th closest receiver and

$$P_{(n)} = \Pr\left\{\gamma_{(n)} \geq \beta\right\}, \tag{8}$$

is the conditioning coverage probability where $\gamma_{(n)}$ is denoted as the received SINR for the receiver which is the n-th closest receiver.

The probability of the typical receiver being the n-th closest receiver Q_n can be obtained by the following lemma.

Lemma 1: The probability of the typical receiver being the n-th closest receiver can be expressed as

$$\begin{aligned} Q_n &= \Pr\{X_0 = X^{(n)}\} \\ &= C_{N-2}^{n-1} \left(\frac{1}{2}\right)^{N-2} \end{aligned} \tag{9}$$

Proof: See Appendix A. □

Q_n is the probability of the typical receiver being the n-th closest receiver associated with the number of active users within each NOMA cluster and the ordering result based on distance between typical receiver and typical transmitter.

In order to get more insight analytical expression of SINR, we will find $\gamma_{(n)}$, including $S_{(n)}$, $I_{(n),in}$ and I_{out} subsequently.

1) DESIRED SIGNAL

At typical receiver RX_0 which is the n-th closest receiver, the desired signal from according transmitter TX_0 can be expressed as

$$S_{(n)} = (a^{(n)})^2 P_t \left|h_{T_0,R_0}\right|^2 \left|X^{(n)}\right|^{-\alpha} \tag{10}$$

where P_t refers to the transmit power of the TX_0, $h_{T_0,R_0} \sim \mathcal{CN}(0,1)$ is the small-scale fading coefficient, $\left|X^{(n)}\right|$ is the distance between typical transmitter and the typical receiver and $(a^{(n)})^2$ is the power allocation coefficient of typical receiver which is n-th closest receiver.

2) INTRA-CLUSTER INTERFERENCE

At typical receiver RX_0, the number of active NOMA receivers is $N-1$, while the intra-cluster interference is from other users with worse channel gain within the same FH-NOMA cluster.

$$I_{(n),in} = \sum_{i=1}^{n-1} (a^{(i)})^2 P_t \left|h_{T_0,R_0}\right|^2 \left|X^{(n)}\right|^{-\alpha} \tag{11}$$

where P_t refers to the signal power of the TX_0, $h_{T_0,R_0} \sim \mathcal{CN}(0,1)$ is the small-scale fading coefficient, and $\left|X^{(n)}\right|$ is the distance between typical transmitter and the typical receiver. $(a^{(i)})^2$ $(1 \leq i \leq n-1)$ is the power allocation coefficient of i-th closest receiver which has worse channel gain compared to typical receiver.

3) INTER-CLUSTER INTERFERENCE

The interference is from transmitters which reuse the same TFB in other FH-NOMA clusters.

$$I_{out} = \sum_{k=1}^{M-1} I_{TX_k \to RX_0} = \sum_{k=1}^{M-1} P_t |g_k|^2 |Y_k|^{-\alpha} \phi_k \tag{12}$$

where P_t is the transmit power from other transmitter users TX_k which reuse the same frequency point in other clusters, $g_k \sim \mathcal{CN}(0,1)$ is the small-scale fading coefficient, and $|Y_k|$ $(1 \leq k \leq \lambda\pi R_c^2)$ refers to the distance between the transmitters TX_k and the typical receiver RX_0. ϕ_k is the probability of successful frequency collision with typical cluster. In (12), $\phi_k = \frac{1}{f}$, where f is the number of available frequency points. The average number of FH-NOMA clusters working simultaneously in the system is M, and the other $M-1$ clusters are possible interference sources.

By applying (10), (11) and (12) into (8), we rewrite in detailed expression as follows:

$$\Pr\left\{\gamma_{(n)} \geq \beta\right\} = \Pr\left\{\left|h_{T_0,R_0}\right|^2 \geq \frac{\beta(I_{out} + \sigma^2)}{P_t \left|X^{(n)}\right|^{-\alpha} \Theta_n}\right\}, \tag{13}$$

where $\Theta_n = (a^{(n)})^2 - \beta \sum_{i=1}^{n-1} (a^{(i)})^2$ for $1 \leq n \leq N$, $\beta_n = 2^{\eta_n} - 1$, η_n is the target data rate for the n-th closest user, $\varepsilon_n = \frac{\beta_n}{\Theta}$, and $\beta = \max\{\beta_1, \beta_2, \cdots, \beta_{N-1}\}$. The condition $((a^{(n)})^2 - \beta \sum_{i=1}^{n-1} (a^{(i)})^2 > 0$ should be satisfied due to applying NOMA protocol, otherwise the coverage probability will always be 0 [33]. Hence,

$$\begin{aligned} \Pr(\gamma_{(n)} \geq \beta) &= E_{I_{out}, |X^{(n)}|}\left(e^{-f(I_{out}, |X^{(n)}|)}\right) \\ &= E_{|X^{(n)}|}\left(L_{I_{out}}(s) \cdot e^{-\frac{W_n}{P_t}\sigma^2}\right), \end{aligned} \tag{14}$$

where $f(I_{out}, \left|X^{(n)}\right|) = \frac{\beta(I_{out}+\sigma^2)}{P_t \left|X^{(n)}\right|^{-\alpha}\left((a^{(n)})^2 - \beta \sum_{i=1}^{n-1}(a^{(i)})^2\right)}$, $W_n = \varepsilon_n \left|X^{(n)}\right|^{\alpha}$, $s = \frac{W_n}{P_t}$, $E_{|X^{(n)}|}$ is relied on the pdf of ordered distance $|X|$. To obtain more insightful expressions, we express Laplace transforms of inter-cluster interference I_{out} at first, which is shown in the following lemma.

Lemma 2: The Laplace transform of inter-cluster interference for a typical receiver can be expressed as

$$L_{I_{out}}(s)=\exp\left\{-\frac{\pi\lambda\,(\phi\beta)^{\delta}\,|X_n|^2}{sinc(\delta)\left((a^{(n)})^2-\beta\sum_{i=1}^{n-1}(a^{(i)})^2\right)^{\delta}}\right\}, \quad (15)$$

where $s=\frac{W_n}{P_t}$, $W_n=\varepsilon_n\left|X^{(n)}\right|^{\alpha}$, β *is the pre-determined SINR threshold.*

Proof: See Appendix B. □

We turn our attention to the PDF of ordered distance $X^{(n)}$, which is given in the following lemma.

Lemma 3: Assuming that receivers $N-1$ *are randomly and uniformly positioned in the disc D served by the same transmitter shown in Fig. 1, the PDF of* $\left|X^{(n)}\right|$ *as follows:*

$$f_{|X^{(n)}|}(x)=\sum_{i=0}^{N-n-1}\frac{2(N-1)!}{(n-1)!(N-n-1)!}\times C_{N-n-1}^{i}(-1)^{N-n-i-1}\frac{x^{2N-2i-3}}{D^{2N-2i-2}} \quad (16)$$

Proof: See Appendix C. □

We rewrite (14) to obtain more insightful expressions as

$$\begin{aligned}P(\beta)&=\int\Pr\{\gamma_{(n)}\geq\beta\}f_{|X^{(n)}|}(x)dx\\&=\int_0^D\exp\left(-\frac{\pi\lambda\,(\phi\varepsilon_n)^{\delta}}{sinc(\delta)}\left|X^{(n)}\right|^2-\frac{\varepsilon_n}{\rho}\left|X^{(n)}\right|^{\alpha}\right)\\&\quad\times f_{|X^{(n)}|}(x)dx\end{aligned} \quad (17)$$

where $\rho=\frac{P_t}{\sigma^2}$, which is the transmit signal to noise ratio (SNR), assuming $\sigma_1^2=\sigma_2^2=\cdots=\sigma_{N-1}^2=\sigma^2$ and the PDF of $f_{|X^{(n)}|}(x)$ is given by Lemma 3.

Based on the results of (9), (15), (17) and Lemma 3, after some further mathematical manipulations, we can express the coverage probability of a typical receiver according to the following theorem:

Theorem 1: Assuming that the NOMA clusters position obeys the homogeneous passion point processes (PPPs), which is denoted by Φ *associated with the density* λ, $N-1$ *users are uniformly and randomly distributed within the disc, the coverage probability of a typical receiver in the typical cluster is given by*

$$\begin{aligned}P(\beta)&=\sum_{n=1}^{N-1}(\frac{1}{2})^{N-1}\left(C_{N-2}^{n-1}\right)^2\times(N-1)\\&\quad\times\int_0^D\sum_{i=0}^{N-n-1}\frac{(-1)^{N-n-i-1}C_{N-n-1}^{i}}{D^{2N-2i-2}}\\&\quad\times e^{z(x,\beta)}x^{2N-2i-3}dx,\end{aligned} \quad (18)$$

where $z(x,\beta)=-\frac{\pi\lambda(\phi\varepsilon_n)^{\delta}}{sinc(\delta)}x^2-\frac{\varepsilon_n}{\rho}x^{\alpha}$.

Proof: See Appendix D. □

From the results of Theorem 1, the coverage probability is a monotonically decreasing function of the density of FH-NOMA clusters λ, the FH-NOMA cluster radius D, while a monotonically increasing function of the SNR ρ and the number of available frequency points f. Hence, increasing average number of active FH-NOMA clusters and the number of frequency points, and densely deploying the NOMA receivers around each transmitter can degrade the performance of coverage probability. Moreover, increasing the transmit power at each transmitter can enhance the performance of coverage probability in the case of a certain AWGN power. Some results are consistent with our qualitative analysis that the more active FH-NOMA clusters and the less available frequency points will introduce more inter-interference.

B. AVERAGE DATA RATE

Based on the analytical results for the coverage probability in (18), the average data rate is defined as

$$\overline{R}=Q_1R_{(1)}+\cdots+Q_nR_{(n)}+\cdots+Q_{N-1}R_{(N-1)}, \quad (19)$$

where Q_n is the probability of the typical receiver being the n-th closest receiver obtained in (9). $R_{(n)}=\Pr(\gamma_{(n)}\geq\beta)\times\log_2(1+\beta)$ is the average data rate given the typical receiver as the n-th closest receiver.

In addition to analyzing the coverage probability, we will analyze the average data rate referred to (19). It can be given by

$$\begin{aligned}\overline{R}&=\sum_{n=1}^{N-1}\left(\frac{1}{2}\right)^{N-1}\left(C_{N-2}^{n-1}\right)^2\times(N-1)\\&\quad\times\int_0^D\sum_{i=0}^{N-n-1}\frac{(-1)^{N-n-i-1}C_{N-n-1}^{i}}{D^{2N-2i-2}}\\&\quad\times e^{z(x,\beta)}\log_2(1+\beta)x^{2N-2i-3}dx\end{aligned} \quad (20)$$

From (20), the average data rate of FH-NOMA users has relationship with a given threshold β, which is positively correlated with the target rate. It shows that the average data rate performance of each user can be enhanced through adjusting the FH-NOMA cluster radius D, the density of clusters and the number of available frequency points f. What's more, the user power allocation strategy and threshold selection can be reserved for further consideration.

IV. NUMERICAL RESULTS AND DISCUSSION

In this section, we numerically evaluate the coverage probability and further analyze the impact of the key system parameters. Simulation results are also presented with Monte Carlo methods in a circle region with radius $R_c=2.5$ km. The bandwidth is $BW=10$ MHZ as one of most common setting-ups for Ad Hoc network. The thermal noise in dBm level is calculated as $\sigma^2=-174+10\log_{10}(BW)$. The table 1 provides the default system parameters. In addition, the default power allocation coefficient ratio between users is 0.4.

Fig. 3 plots the coverage probability decreases with larger NOMA cluster radius D, which is consistent with our analytical result. In addition, the coverage probability decreases

TABLE 1. System parameters.

Parameter	Value	Description
λ	$\frac{5}{\pi 2500^2}$	Density of NOMA clusters
N	5	Number of users within a single cluster
D	200 m	NOMA cluster radius
fN	8	Number of frequency points
P_t	30 dBm	Transmission power of each TU
σ^2 $(10MHz)$	-104 dBm	Thermal noise power
α	4	Path loss exponent
β	2 dB	SINR threshold

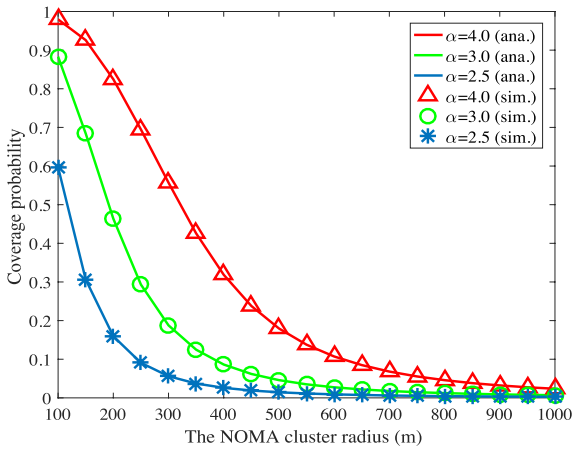

FIGURE 3. Coverage probability with different cluster radius *D* and different path loss exponent α.

more slowly with the rise of path loss exponent. Since the main interference change is from intra-cluster interference in this case. For a specific SINR threshold β and a typical NOMA system, longer distances means larger path loss while larger path loss exponent brings faster drop of inter-interference, hence the coverage probability decreases more slowly.

The impact of the number of available frequency points is presented in Fig. 4, it shows that the simulations match well with the analytical results, which verifies the accuracy of the theoretical analysis. It can be seen that the coverage probability increases with the number of frequency points. However, with the fixed number of active FH-NOMA clusters working simultaneously, when the number of frequency points is large enough, the coverage probability is almost full-loaded. In addition, the coverage probability increases with the rise of path loss exponent. This is because the number of frequency points mainly affects the probability of inter-cluster interference occurrence.

Fig. 5 shows the relationship between the coverage probability and the density of FH-NOMA clusters. It can be seen that the coverage probability decreases with the average number of active FH-NOMA cluster. Moreover, the fluctuation of coverage probability with density change of FH-NOMA clusters is relatively smaller, with the rise of the path loss exponent. As the density of FH-NOMA clusters increases,

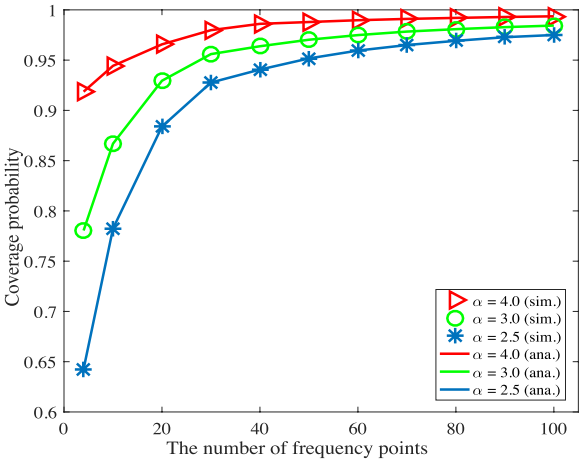

FIGURE 4. Coverage probability with different number of frequency points *f* and different path loss exponent α.

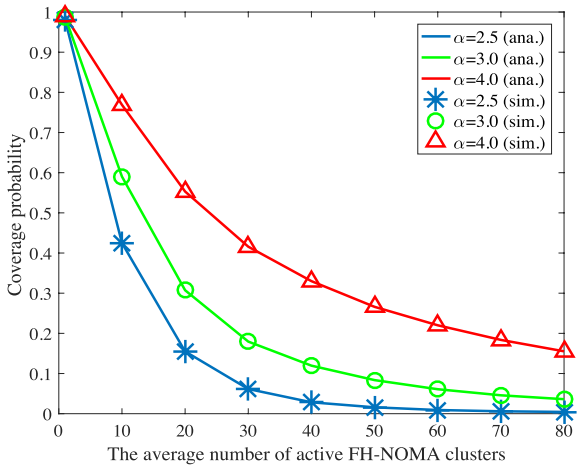

FIGURE 5. Coverage probability with different the average number of active FH-NOMA cluster $\lambda\pi R_c^2$ and different path loss exponent α.

the inter-cluster interference becomes more serious when the average number of FH-NOMA clusters reaches upper bound of supported links. In addition, the larger path loss exponent causes smaller impact of inter-cluster interference.

To further study the impact of the density of FH-NOMA cluster and the number of frequency points, Fig. 6 shows the optimal $M = \lambda\pi R_c^2$ *w.r.t* the number of frequency points. It can be seen that with different number of frequency points, the system capacity exhibits a bell curve relationship *w.r.t* the density of FH-NOMA clusters and the optimal density of FH-NOMA clusters always exists such that the system capacity can be maximized. Meanwhile, the capacity first increases and then deteriorates with the increasing of the density of FH-NOMA clusters. Fig. 6 validates the theoretical analysis that there is a tradeoff between the number of frequency points and the density of FH-NOMA clusters for the system capacity. For a fixed number of frequency points, the optimal density of FH-NOMA cluster is close to the maximum number of supported links. Since the number of available frequency points can limit the upper bound of supported links.

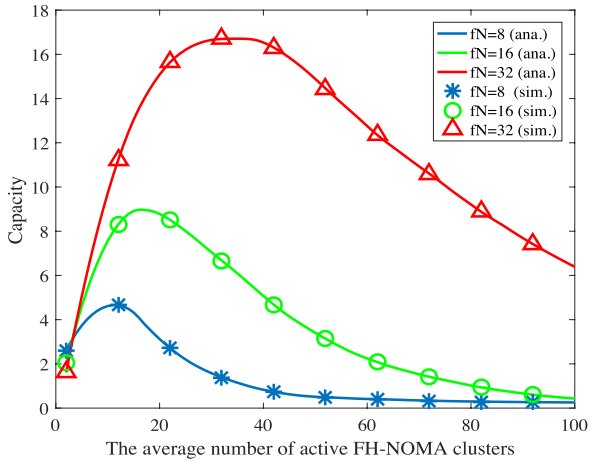

FIGURE 6. System capacity with different the average number of active FH-NOMA cluster $\lambda\pi R_c^2$ and different number of frequency points where $\alpha = 3$.

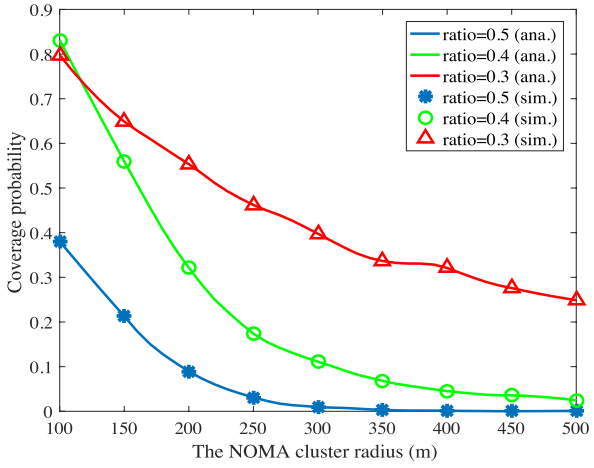

FIGURE 7. Coverage probability with different the NOMA cluster radius and different user allocation coefficients, where $\alpha = 4$.

When the density of NOMA cluster increases, the frequency collision is relatively small while when the number of NOMA clusters reach the maximum supported links, the system capacity suddenly decreases.

Fig. 7 plots the coverage probability of the FH-NOMA cluster radius with different user power allocation coefficient. The figure shows precise agreement between the simulation and analytical curves. The power is allocated by equal ratios between users based on channel ordering and satisfy the previous assumption that $|a_1|^2 + |a_2|^2 + \cdots + |a_n|^2 + \cdots + |a_{N-1}|^2 = 1$. The red curve use ratio 0.3 and the number of each NOMA cluster is 5, i.e., $|a^{(1)}|^2 = \frac{0.4^3}{1+0.4^1+0.4^2+0.4^3}$, $|a^{(2)}|^2 = \frac{0.4^2}{1+0.4^1+0.4^2+0.4^3}$ $\cdots\cdots$. One can observe that the coverage probability has relationship with different user power allocation coefficient methods. When the power between users is relatively close, the lower coverage probability is achieved, which is due to NOMA protocol. Moreover, an optimal user power allocation method can be studied in future work.

V. CONCLUSION

In this paper, the downlink transmission performance of frequency hopping Ad Hoc communication system with NOMA protocol was analyzed. Importantly, we used stochastic geometry and order statistics for modeling the locations of NOMA clusters and the users within each NOMA cluster, based on the practical scenario of the emergency communication system combined with squad combat. Additionally, new analytical coverage probability and average data rate were derived for characterizing the system's performance in above scenarios. It was analytically demonstrated that the coverage probability was determined by the radius of FH-NOMA cluster, the number of frequency points and the density of FH-NOMA clusters. Monte Carlo simulation results were used to verify the analysis. It was concluded that the coverage probability can be improved by reducing the radius of each NOMA clusters and appropriately increasing in the number of frequency. Since the number of the frequency points directly determine the number of supported links which limits the cluster density. For a given number of frequency points, the cluster density cannot be increased without limitation. When the number of clusters working simultaneously within a limited space is close to the number of supported links, coverage probability will suddenly drop below 50%. From the perspective of expressions, the power allocation between users will also have an impact. In the following work, it can be analyzed to bring the best performance. Our results can provide guidelines for our real deployment of the emergency communication system.

APPENDIX A
PROOF OF LEMMA 1

The probability of the typical receiver being the n-th closest receiver can be expressed as

$$\begin{aligned} Q_n &= \Pr(RX_0 \textit{ is the } n \textit{ th closest user}) \\ &= \Pr(X_0 \geq X_1, X \geq X_2, \cdots, X_0 \geq X_{n-1}, X_0 \leq X_n, \\ &\quad \cdots, X_0 \leq X_{N-2}) \\ &\overset{(a)}{=} \Pr(X_0 \geq X_1) \times \Pr(X_0 \geq X_2) \times \cdots \times \Pr(X_0 \leq X_n) \\ &\quad \times \cdots \times \Pr(X_0 \leq X_{N-2}) \\ &\overset{(b)}{=} C_{N-2}^{n-1} \left\{ \int_0^D \left(\int_0^x \frac{2r}{D^2} dr \right) \frac{2x}{D^2} dx \right\}^{n-1} \\ &\quad \times \left\{ 1 - \int_0^D \left(\int_0^x \frac{2r}{D^2} dr \right) \frac{2x}{D^2} dx \right\}^{N-n-1} \\ &= C_{N-2}^{n-1} \left(\frac{1}{2} \right)^{N-2}, \end{aligned} \tag{A.1}$$

where (b) is applied with the probability distribution function (PDF) given by (1). Since the random variables are independent and identically distributed for each receiver, we can rewrite the expression as (a). The distance X_0 represents the distance between typical receiver and typical transmitter and incremental ordering distance sets except for the distance between typical receiver and typical transmitter $\boldsymbol{X}$ are given

above. $X_n \in \boldsymbol{X}$ represents the distance between n-th closest receiver and transmitter. The re-ordered set $\boldsymbol{X'}$ based on the order statistics is obtained. Hence, we can obtain the probability of the typical receiver being the n-th closest receiver as (9), the proof is completed.

APPENDIX B
PROOF OF LEMMA 2

The Laplace transform of inter-cluster interference for a typical receiver can be expressed as

$$\begin{aligned} L_{I_{out}}(s) &= E\left(\prod_{X\in\Phi} e^{-sI_{out}}\right) \\ &= E\left(\prod_{X\in\Phi} e^{-sP_t h\phi\ell(x)}\right) \\ &= E_\Phi\left(\prod_{X\in\Phi} E_h(e^{-sP_t h\phi\ell(x)})\right) \\ &= \int_0^\infty \{1-exp(-sP_t h\phi\ell(r))\}\cdot\lambda(r)dr \\ &\overset{(a)}{=} \lambda c_d\int_0^\infty \{1-exp(-sP_t h\phi/y)\}\cdot\delta y^{\delta-1}dy \\ &\overset{(b)}{=} \lambda c_d\int_0^\infty \{1-exp(-sP_t h\phi x)\}\,\delta x^{-\delta-1}dx \\ &= \lambda c_d(sP_t h\phi)^\delta\Gamma(1-\delta), \quad 0<\delta<1,\ \delta=\frac{d}{\alpha}, \end{aligned} \tag{B.1}$$

where (a) is $\delta = \frac{d}{\alpha}$, $y = r^{-\frac{1}{\alpha}}$ and (b) is $x = y^{-1}$. We assume that the point process Φ has the intensity measure $\Lambda(0,r) = \lambda c_d r^d$ and intensity function $\lambda'(r) = \lambda c_d d r^{d-1}$, where d $= 2$ and c_d is the volume of the d-dimensional unit ball. In addition, we have $\ell(x) = |x|^{-\alpha}$. Mapping the homogeneous Poisson point process (PPP) to the one dimension, we use the pgfl for $\upsilon(r) = E_h(e^{-sP_t\phi h\ell(r)})$ to obtain $L(s) = exp\left\{-\int_0^\infty E_h\left(1-e^{-sP_t\phi h\ell(r)}\right)\lambda(r)dr\right\}$ for the one dimensional PPP conditioned on h we have.

With the expectation over h, we can obtain $L(s) = exp\left(-\lambda c_d E(h^\delta)\Gamma(1-\delta)(sP_t\phi)^\delta\right)$. So with fading the interference has a stable distribution with exponent δ ($\delta = \frac{d}{\alpha}$). In the Rayleigh fading, h is exponential with $E(h) = 1$. Since $E(h^\delta) = \Gamma(1+\delta)$ and $L(s) = exp\left(-\lambda c_d\Gamma(1+\delta)\Gamma(1-\delta)(sP_t\phi)^\delta\right)$, we can obtain

$$\begin{aligned} L(s) &= exp\left(-\lambda c_d(sP_t\phi)^\delta\cdot\frac{\pi\delta}{sin(\pi\delta)}\right) \\ &= exp\left(-\frac{\lambda c_d(sP_t\phi)^\delta}{sinc(\delta)}\right), \end{aligned} \tag{B.2}$$

where $\delta = \frac{d}{\alpha} = \frac{2}{\alpha}, 0<\delta<1$. Based on $C_0 = 1$ and $C_d = \frac{\pi^{\frac{d}{2}}}{\Gamma(\frac{d}{2}+1)} = \prod_{j=1}^d\int_0^\pi(sint)^j dt, (d\in Z_+)$, we get $C_2 = \frac{\pi}{\Gamma(2)} = \pi$. Applying (12) and $\delta = \frac{2}{\alpha}$, the Laplace transform of inter-cluster interference can be given by

$$\begin{aligned} L_{I_{out}}(s) &= exp\left\{-\frac{\pi\lambda(W_n\phi)^\delta}{sinc(\delta)}\right\} \\ &= exp\left\{-\frac{\pi\lambda(\phi\varepsilon_n)^\delta\left|X^{(n)}\right|^{\alpha\delta}}{sinc(\delta)}\right\} \\ &= exp\left\{\frac{-\pi\lambda(\phi\beta)^\delta\left|X^{(n)}\right|^2}{sinc(\delta)\left[\left(a^{(n)}\right)^2-\beta\sum_{i=1}^{n-1}\left(a^{(i)}\right)^2\right]^\delta}\right\} \end{aligned} \tag{B.3}$$

We obtain the Laplace transform of inter-cluster interference $L_{I_{out}}(s)$ as (15), the proof is completed.

APPENDIX C
PROOF OF LEMMA 3

$X_1,\cdots,X_{N-1} \in \boldsymbol{X}$ are N-1 jointly distributed random variables from an absolutely continuous population with probability density function(pdf) $f(x)$ obtained in (1) and cumulative distribution function (CDF) $F(x)$.The corresponding order statistics are the X_i's arranged in nondecreasing order. The smallest of the X_i's is denoted by $X_{1:N-1}$ and with order observation from N-1 observations is denoted by $X_{i,N-1}$. Let $X_{1:N-1} \le X_{2:N-1} \le \cdots \le X_{n:N-1} \le \cdots \le X_{N-1:N-1}$ be the order statistics obtained by arranging the preceding random sample in nondecreasing order of magnitude. We can obtain

$$\begin{aligned} &P(x<X_{n:N-1}<x+\Delta x) \\ &= C_{N-1}^1F(x)\cdot C_{N-2}^{k-1}[F(x)]^{n-1}(1-F(x+\Delta x))^{N-n-1} \\ &= \frac{(N-1)!}{(n-1)!(N-n-1)!}\{F(x)\}^{n-1} \\ &\quad\times\{1-F(x+\Delta x)\}^{N-n-1} \\ &\quad\times\{F(x+\Delta x)-F(x)\}+o((\Delta x)^2) \end{aligned} \tag{C.1}$$

$$\begin{aligned} &f_{n:N-1}(x) \\ &= \lim_{\Delta x\to 0}\frac{P(x<X_{n:N-1}<x+\Delta x)}{\Delta x} \\ &= \frac{(N-1)!}{(n-1)!(N-n-1)!}\{F(x)\}^{n-1} \\ &\quad\times\{1-F(x)\}^{N-n-1}f(x) \\ &= C_{N-2}^{n-1}\cdot(N-1)\cdot\frac{2x^{2n-1}}{D^{2n}}\cdot\left(1-\frac{x^2}{D^2}\right)^{N-n-1} \\ &\quad\left(1-\frac{x^2}{D^2}\right)^{N-n-1} \\ &= C_{N-n-1}^0\left(-\frac{x^2}{D^2}\right)^{N-n-1} \\ &\quad+C_{N-n-1}^1\left(-\frac{x^2}{D^2}\right)^{N-n-2}+\cdots \\ &\quad+C_{N-n-1}^{N-n-2}\left(-\frac{x^2}{D^2}\right)^1+C_{N-n-1}^{N-n-1}\left(-\frac{x^2}{D^2}\right)^0 \end{aligned} \tag{C.2}$$

(C.3)

$$f_{n:N-1}(x) = \sum_{i=0}^{N-n-1} \frac{2(N-1)!}{(n-1)!(N-n-1)!} \times C_{N-n-1}^{i}(-1)^{N-n-i-1}\frac{x^{2N-2i-3}}{D^{2N-2i-2}}, \quad \text{(C.4)}$$

where $x \in (0, D)$, $1 \le n \le N-1$. Note that D is the radius of the FH-NOMA clusters shown in Fig. 1, N is the number of users in a single cluster and n represents the receiver with the n-th closest to the TX_0. We denote $f_{n:N-1}(x)$ as $f_{|X^{(n)}|}(x)$, which is PDF of the n-th closest distance $|X^{(n)}|$ between transmitter and receiver. The proof is completed.

APPENDIX D
PROOF OF THEOREM 1

By invoking Lemma 3 and (17), we obtain

$$\begin{aligned}\Pr(\gamma_{(n)} \ge \beta) &= \int_0^D \exp\left(-\frac{\pi\lambda(\phi\varepsilon_n)^{\delta}}{sinc(\delta)}x^2 - \frac{\varepsilon_n}{\rho}x^{\alpha}\right) \\ &\quad \times \sum_{i=0}^{N-n-1}\frac{2(N-1)!}{(n-1)!(N-n-1)!} \\ &\quad \times C_{N-n-1}^{i}(-1)^{N-n-i-1}\frac{x^{2N-2i-3}}{D^{2N-2i-2}}dx \quad \text{(C.5)}\\ P(\beta) &= Q_1P_{(1)} + \cdots + Q_nP_{(n)} + \cdots + Q_{N-1}P_{(N-1)} \\ &= \sum_{n-1}^{N-1} Q_n \Pr(\gamma_{(n)} \ge \beta) \\ &= \sum_{n-1}^{N-1} C_{N-2}^{n-1}\left(\frac{1}{2}\right)^{N-2} \\ &\quad \times \sum_{i=0}^{N-n-1}\frac{2(N-1)!}{(n-1)!(N-n-1)!} \\ &\quad \times \int_0^D \exp\left(-\frac{\pi\lambda(\phi\varepsilon_n)^{\delta}}{sinc(\delta)}x^2 - \frac{\varepsilon_n}{\rho}x^{\alpha}\right) \\ &= \sum_{n=1}^{N-1}\left(\frac{1}{2}\right)^{N-1}\left(C_{N-2}^{n-1}\right)^2 \times (N-1) \\ &\quad \times \int_0^D \sum_{i=0}^{N-n-1}\frac{(-1)^{N-n-i-1}C_{N-n-1}^{i}}{D^{2N-2i-2}} \\ &\quad \times e^{z(x,\beta)}x^{2N-2i-3}dx \quad \text{(C.6)}\end{aligned}$$

The proof is completed.

REFERENCES

[1] X. Fan and Z. Tan, "Simulink implementation of frequency-hopping communication system and follower jamming," in *Proc. IEEE Int. Conf. Automat., Electron. Elect. Eng. (AUTEEE)*, Nov. 2018, pp. 192–195.
[2] E. Fernández de Gorostiza, J. Berzosa, J. Mabe, and R. Cortiñas, "A method for dynamically selecting the best frequency hopping technique in industrial wireless sensor network applications," *Sensors*, vol. 18, no. 2, p. 657, 2018.
[3] J. Dai, D. Guo, and B. Zhang, "A BICM-MD-ID scheme in FFH system for combatting partial-band interference," in *Proc. Int. Conf. Wireless Commun. Signal Process. (WCSP)*, Oct. 2010, pp. 1–4.
[4] C. D. Frank and M. B. Pursley, "Concatenated coding for frequency-hop spread-spectrum with partial-band interference," *IEEE Trans. Commun.*, vol. 44, no. 3, pp. 377–387, Mar. 1996.
[5] H. Quan, H. Zhao, and P. Cui, "Anti-jamming frequency hopping system using multiple hopping patterns," *Wireless Pers. Commun.*, vol. 81, no. 3, pp. 1159–1176, 2015.
[6] M. A. Khan and D. Shao, "System capacity analysis of hybrid DS/SFH spread spectrum multiple access communication system with BFSK modulation using genetic algorithm," in *Proc. Pakistan Sect. Multitopic Conf.*, Dec. 2005, pp. 1–6.
[7] Y. Liu, Z. Qin, M. Elkashlan, Z. Ding, A. Nallanathan, and L. Hanzo, "Nonorthogonal multiple access for 5G and beyond," *Proc. IEEE*, vol. 105, no. 12, pp. 2347–2381, Dec. 2017.
[8] S. Tachikawa and T. Maeda, "FH/MFSK lump likelihood ratio decision method and its application for PLC," in *Proc. IEEE Int. Symp. Power Line Commun. Appl.*, Apr. 2008, pp. 239–243.
[9] B. Pan, J. Feng, Q. Li, and Q. Tao, "Image communication system based on chaotic FH-OFDM technique," in *Proc. IEEE 3rd Int. Conf. Broadband Netw. Multimedia Technol. (IC-BNMT)*, Oct. 2010, pp. 546–550.
[10] X.-G. Yuan and G.-C. Huang, "Frequency assignment in military synchronous FH networks with cosite constraints," in *Proc. IEEE Int. Symp. Knowl. Acquisition Modeling Workshop*, Dec. 2008, pp. 655–658.
[11] X. Tian and J. Lu, "Performance of Bluetooth FH communication system based on general quadratic prime code," in *Proc. IEEE 2nd Int. Conf. Netw. Infrastruct. Digit. Content*, Sep. 2010, pp. 145–148.
[12] Q. Xiaoqiang, L. Yongxiang, and C. Yong, "Adjacent frequency interference analysis for frequency-hopping radio networks," in *Proc. 5th Int. Conf. Instrum. Meas., Comput., Commun. Control (IMCCC)*, Sep. 2015, pp. 589–592.
[13] Z.-M. Li, "Error probabilities for frequency-hopping spread spectrum multiple access (FH-SSMA) systems in the presence of interference," in *Proc. IEEE 2nd Int. Symp. Spread Spectr. Techn. Appl. (ISSTA)*, Nov. 1992, pp. 127–130.
[14] H. El Gamal and E. Geraniotis, "Comparing the capacities of FH/SSMA and DS/CDMA networks," in *Proc. IEEE 9th Int. Symp. Pers., Indoor Mobile Radio Commun.*, vol. 2, Sep. 1998, pp. 769–773.
[15] C. Ding, M. J. Moisio, and J. Yuan, "Algebraic constructions of optimal frequency-hopping sequences," *IEEE Trans. Inf. Theory*, vol. 53, no. 7, pp. 2606–2610, Jul. 2007.
[16] J. Zou and X. Cao, "Synchronization scheme of FH-OFDM in ad hoc physical layer," in *Proc. IEEE 12th Int. Conf. Commun. Technol.*, Nov. 2010, pp. 1307–1310.
[17] M. Zhao, M. Xu, J. Zhong, and S. Li, "Slot synchronization in ad hoc networks based on frequency hopping synchronization," in *Proc. Int. Conf. Wireless Commun., Netw. Mobile Comput.*, Sep. 2006, pp. 1–4.
[18] F. Li, Z. Li, D. Lou, and Y. Jiang, "Analysis and research of synchronization technique for frequency-hopping communication systems," in *Proc. Int. Conf. Comput. Sci. Netw. Technol.*, vol. 3, Dec. 2011, pp. 1968–1972.
[19] K. L. Sudha and R. Rao, "Performance improvement of FH CDMA signals using rate compatible parallel concatenated block codes," in *Proc. Int. Conf. Signal Process., Commun. Netw.*, Feb. 2007, pp. 102–105.
[20] Z. Ding, Y. Liu, J. Choi, Q. Sun, M. Elkashlan, C.-L. I, and H. V. Poor, "Application of non-orthogonal multiple access in LTE and 5G networks," *IEEE Commun. Mag.*, vol. 55, no. 2, pp. 185–191, Feb. 2017.
[21] A. Benjebbour, Y. Saito, Y. Kishiyama, A. Li, A. Harada, and T. Nakamura, "Concept and practical considerations of non-orthogonal multiple access (NOMA) for future radio access," in *Proc. Int. Symp. Intell. Signal Process. Commun. Syst. (ISPACS)*, Nov. 2013, pp. 770–774.
[22] Z. Chen, Z. Ding, X. Dai, and R. Zhang, "An optimization perspective of the superiority of NOMA compared to conventional OMA," *IEEE Trans. Signal Process.*, vol. 65, no. 19, pp. 5191–5202, Oct. 2017.
[23] Y. Liu, Z. Ding, M. Elkashlan, and J. Yuan, "Nonorthogonal multiple access in large-scale underlay cognitive radio networks," *IEEE Trans. Veh. Technol.*, vol. 65, no. 12, pp. 10152–10157, Dec. 2016.
[24] T. N. Do, D. B. da Costa, T. Q. Duong, and B. An, "Improving the performance of cell-edge users in NOMA systems using cooperative relaying," *IEEE Trans. Commun.*, vol. 66, no. 5, pp. 1883–1901, May 2018.
[25] P. Swami, V. Bhatia, S. Vuppala, and T. Ratnarajah, "User fairness and performance enhancement for cell edge user in NOMA-HCN with offloading," in *Proc. IEEE 85th Veh. Technol. Conf. (VTC Spring)*, Jun. 2017, pp. 1–5.

[26] S. Timotheou and I. Krikidis, "Fairness for non-orthogonal multiple access in 5G systems," *IEEE Signal Process. Lett.*, vol. 22, no. 10, pp. 1647–1651, Oct. 2015.
[27] Q. Sun, S. Han, C. L. I, and Z. Pan, "On the ergodic capacity of MIMO NOMA systems," *IEEE Wireless Commun. Lett.*, vol. 4, no. 4, pp. 405–408, Aug. 2015.
[28] Y. Liu, Z. Qin, M. Elkashlan, A. Nallanathan, and J. A. McCann, "Non-orthogonal multiple access in large-scale heterogeneous networks," *IEEE J. Sel. Areas Commun.*, vol. 35, no. 12, pp. 2667–2680, Dec. 2017.
[29] Y. Liu, Z. Ding, M. Elkashlan, and H. V. Poor, "Cooperative non-orthogonal multiple access with simultaneous wireless information and power transfer," *IEEE J. Sel. Areas Commun.*, vol. 34, no. 4, pp. 938–953, Apr. 2016.
[30] Y. Liu, Z. Qin, M. Elkashlan, Y. Gao, and L. Hanzo, "Enhancing the physical layer security of non-orthogonal multiple access in large-scale networks," *IEEE Trans. Wireless Commun.*, vol. 16, no. 3, pp. 1656–1672, Mar. 2017.
[31] Q. Cui, X. Yu, Y. Wang, and M. Haenggi, "The SIR meta distribution in Poisson cellular networks with base station cooperation," *IEEE Trans. Commun.*, vol. 66, no. 3, pp. 1234–1249, Mar. 2018.
[32] C. Pöpper, M. Strasser, and S. Capkun, "Anti-jamming broadcast communication using uncoordinated spread spectrum techniques," *IEEE J. Sel. Areas Commun.*, vol. 28, no. 5, pp. 703–715, Jun. 2010.
[33] Z. Yang, Z. Ding, P. Fan, and G. K. Karagiannidis, "On the performance of non-orthogonal multiple access systems with partial channel information," *IEEE Trans. Commun.*, vol. 64, no. 2, pp. 654–667, Feb. 2016.

SHAOSHENG LI received the B.S. and M.S. degrees in radio engineering from the Beijing University of Posts and Telecommunications (BUPT), and the Ph.D. degree in signal and information processing from BUPT, in 2011. His research interests include SDR communications, cognitive radio, and Ad Hoc networks.

HONGRUI NIE received the B.S. degree from the Beijing University of Posts and Telecommunications, Beijing, China, in 2014 and 2018, respectively, where she is currently pursuing the master's degree. Her research interests include Ad Hoc network, routing protocol, 5G wireless network, stochastic geometry, and the Internet of Things. She received the National Scholarship, the Meritorious Winner in the Interdisciplinary Contest in Modeling, a Merit Student of BUPT, and the Beijing Outstanding Graduates.

HUICI WU received the B.S. degree in communication engineering from Communication University of China, Beijing, China, in 2013, and the Ph.D. degree in information and communication engineering from the Beijing University of Posts and Telecommunications (BUPT), Beijing, in 2018. From 2016 to 2017, she was visiting the Broadband Communications Research (BBCR) Group, Department of Electrical and Computer Engineering, University of Waterloo, Waterloo, ON, Canada. She is currently an Assistant Professor with the School of Cyberspace Security, BUPT. Her research interests are in the area of wireless communications and networks, with the current emphasis on the collaborative transmission in air-to-ground integrated networks and physical layer security. She has served as the publication Co-Chair of the APCC 2018 and a TPC Member of the IEEE ICC 2019.